Science of the Total Environment 957 (2024) 177715

Contents lists available at ScienceDirect

Science of the Total Environment

journal homepage: www.elsevier.com/locate/scitotenv

Delineating distinct sediment pollution signatures from diverse sources in a heavily contaminated estuary near an area of high cancer and cardiovascular mortality

Manuel Contreras-Llanes [a,b,*], Vanessa Santos-Sánchez [a], Juan Alguacil [a,b], Jesús M. Castillo [c]

[a] Research Group on Clinical, Environmental Epidemiology and Social Transformation (EPICAS), Department of Sociology, Social Work and Public Health, University of Huelva (UHU), 21007 Huelva, Spain
[b] Research Center on Natural Resources, Health and Environment (RENSMA), University of Huelva (UHU), 21007 Huelva, Spain
[c] Department of Plant Biology and Ecology, University of Seville (US), Ap 1095, 41080 Seville, Spain

HIGHLIGHTS

- Specific pollution signatures were detected for each of the main pollution sources.
- 20 elements including As and Mg were identified as pollution tracers for PG stacks.
- Sediments near mining wastes specially cumulated 6 elements, including Fe and Mn.
- Be and S are suitable pollution tracers for agriculture and AMD-Tinto, respectively.
- We set a starting point to evaluate the impact of the RESTORE 2030 project.

GRAPHICAL ABSTRACT

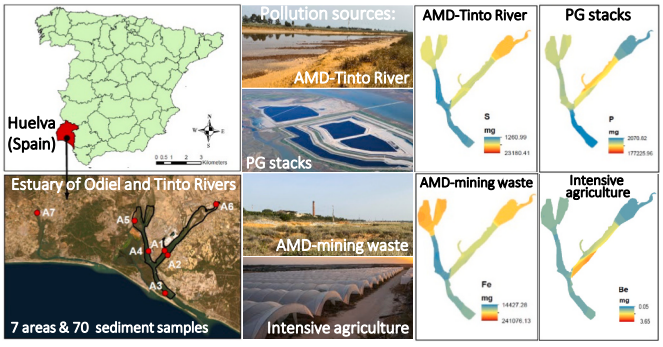

ARTICLE INFO

Editor: Manuel Esteban Lucas-Borja

Keywords:
Acid mine drainage
Odiel-Tinto estuary
Metals
Phosphogypsum
Tidal marshes

ABSTRACT

Our study aimed to identify specific pollution signatures in marsh sediments using geochemical tracers in the highly polluted Odiel–Tinto Estuary prior to a planned restoration of the affected marshes. Tidal marshes in this estuary are heavily polluted from different sources such as acid mine drainage, industrial activities (including phosphogypsum stacks) and agricultural runoffs. We analysed the total concentrations of 48 chemical elements, pH, electrical conductivity, redox potential and texture of surface sediments from six marsh areas in the Odiel–Tinto Estuary and one in the adjacent Piedras Estuary. Spatial distribution maps were created using inverse distance weighting to visualise the distribution of elements associated with different pollution sources. We identified a specific pollution signature for PG stacks that distinguishes metal exposure from the other pollution sources in the Odiel–Tinto Estuary, such as acid mine drainage near mining waste deposits, an abandoned foundry and areas under intensive agricultural cultivation. Our results provide a valuable tool for discriminating between pollution sources, quantifying the most impacted areas of the salt marsh, assigning responsibility to the various polluting entities within the estuary, and setting a starting point to evaluate the impact of the RESTORE

* Corresponding author at: Research Group on Clinical, Environmental Epidemiology and Social Transformation (EPICAS), Department of Sociology, Social Work and Public Health, University of Huelva (UHU), 21007 Huelva, Spain.
E-mail address: mcontreras@uhu.es (M. Contreras-Llanes).

https://doi.org/10.1016/j.scitotenv.2024.177715
Received 29 August 2024; Received in revised form 31 October 2024; Accepted 20 November 2024

2030 restoration plan in the Odiel–Tinto Estuary. The specific sediment pollution signatures identified may also be used as a reference to determine the impact of future interventions on existing pollution sources in estuaries or marshes polluted with phosphogypsum.

1. Introduction

There is cumulative evidence linking industrial and mining environmental pollution with health problems, specifically cancer, cardiovascular and respiratory diseases (Briffa et al., 2020). Huelva, a city of 150,000 inhabitants, has high cancer and heart disease mortality rates for both men and women as compared to the rest of Spain (Alguacil et al., 2014; Benach et al., 2003; Lopez-Abente et al., 2001). For instance, the Spanish National Atlas of Mortality shows significantly higher standard mortality ratios in the city of Huelva over the period 1989–2014 among both men and women for bladder cancer, cerebrovascular diseases, acute myocardial infarction, heart failure and other heart diseases, in addition to breast cancer in women) and lung cancer in men (Martínez-Beneito et al., 2024). Environmental pollution may be one of the factors predominately responsible for the excess mortality observed in Huelva city (Alguacil et al., 2014).

In this public health context, Huelva city lies next to the Odiel–Tinto Estuary in the southwestern Iberian Peninsula on the Gulf of Cadiz. This estuary is recognised as one of the most heavily polluted in the world due to a multitude of factors including industrial and mining pollution (Morillo et al., 2008; Sáenz et al., 2003). A confluence of stressors gives the region unique characteristics. The Iberian Pyrite Belt, situated in southwest Iberia, ranks as one of the world's most significant polymetallic sulphide mining districts (Leistel et al., 1998; Pérez-López et al., 2023). The Odiel and Tinto Rivers drain the region from north to south, carrying large amounts of metals and metalloids to the Odiel–Tinto Estuary (Blasco et al., 2000; Santos Bermejo et al., 2003). Significant acid mine drainage (AMD) has occurred for centuries, while large quantities of industrial pollutants have been discharged from various chemical factories since the mid-1960s. Additionally, intensive agricultural practices implemented in the late 1970s have resulted in agrochemical runoff entering the estuary from surrounding farmland (Barba-Brioso et al., 2010). In terms of mass, the most significant pollution problem in the Odiel–Tinto Estuary is phosphogypsum (PG), as roughly 100 million tonnes are currently stored in stacks located on the estuary itself. A waste product from fertilizer production, the PG was stockpiled on unconsolidated salt marsh sediments over a period of 42 years (1968–2010) and now covers 1200 ha in the Tinto marshes (Silva et al., 2022). The PG originates from phosphate rock, which carries trace elements that concentrate within the stacks (Rentería-Villalobos et al., 2010). These stacks contain a multitude of pollutants, such as organic substances, metals, natural radionuclides from the ^{238}U decay series and other potentially toxic elements (P, S, F, NH^{4+}, Fe, Zn, U, Cr, Cu and Cd) and natural radionuclides from the ^{238}U decay series, including the highly radiotoxic ^{226}Ra, ^{210}Po and ^{210}Pb (Lieberman et al., 2020; Pérez-López et al., 2010).

Following a social movement spurred by environmental and health concerns over the proximity of PG stacks to Huelva city, less 500 m, the stockpiling of PG from fertilizer factory activities ended in December-2010 after a judicial complaint. Judiciary authorities also demanded the fertilizer company create a restoration plan for the affected marshes. Despite having been approved by governmental authorities, the proposed plan—called RESTORE 2030 (RESTORE2030, 2020)—has not been approved by the judiciary authorities. An independent committee of national scientific experts coordinated by the University of Huelva concluded that the RESTORE 2030 plan was not adequate to achieve a complete restoration, though it could be a good place to begin while a definite solution is found (Scientific committee, 2022). Baseline data on the impact of the PG stacks would be needed to evaluate the progress of the restoration, including, but not limited to, the impact on the Odiel–Tinto Estuary sediments, taking into account the impact of other active metal pollution sources.

Several studies have investigated the concentration of metals in the sediments of the Odiel–Tinto Estuary, focusing primarily on two key aspects: understanding the processes that govern metal behaviour and pinpointing the areas with the highest levels of contamination (Borrego et al., 2022; Elbaz-Poulichet et al., 1999). Tidal marshes were found to be more contaminated compared to other sedimentary environments like channel margins and subtidal channels. Estuaries and tidal marshes act as natural filters for a wide range of pollutants, including organic compounds, metals and even radioactive isotopes, originating from both point sources and non-point sources (Li et al., 2022; Nie et al., 2018). Once within estuaries, pollutants may undergo partial or complete mixing within sediments but can also segregate into specific zones along the estuarine gradients (Beltrán et al., 2010; Santos Bermejo et al., 2003). This segregation is influenced by the chemical and physical properties of the pollutant, changing environmental conditions within the estuary (particularly pH, salinity and redox potential) and interactions between these factors (Hierro et al., 2014a). Given these complexities, identifying appropriate geochemical tracers is crucial for pinpointing the specific sources of pollution impacting tidal marshes. The PG stacks function as an anthropogenic coastal karst aquifer, allowing for hydraulic connection between the sea, groundwater flow and the underlying sediments, leading to active subsidence (Carro et al., 2021; González, 2022). Additionally, highly concentrated contaminants are released into the estuary via acidic edge outflows (i.e. small streams) emanating from the PG stacks (Millán-Becerro et al., 2023; Pérez-López et al., 2016).

Although comprehensive studies have been conducted on the spatial distribution of heavy metals in other highly polluted locations, the specific pollutant profiles affecting the tidal marshes of this anthropogenically polluted estuary have not yet been characterised in detail (Dong et al., 2024; Liu et al., 2024; Sun et al., 2025). These spatial distributions and environment risk assessments are extremely important for the management and future remediation of this site. As the excess mortality in the Huelva area is compatible with industrial and mining metal pollution and there are multiple exposure sources, it is important to investigate the depositional signatures of heavy metals and metalloids specific to the different pollution sources. Biomonitoring can help assess the potential health risks to Huelva citizens and to the ecosystem. We investigated the spatial distribution of sediment pollution originating from various sources to identify pollution depositional signatures in the Odiel–Tinto Estuary, which is critical to assess the impact of future interventions such as RESTORE 2030.

2. Materials and methods

2.1. Study area

We conducted this study in six low-middle tidal salt marsh areas in the Odiel–Tinto Estuary (A1–6) and one tidal salt marsh in the estuary of the Piedras River (A7), situated in Huelva Province, Spain. These estuaries are located on the Gulf of Cadiz in the Southwest Iberian Peninsula (Fig. 1). The region has a Mediterranean climate influenced by the Atlantic Ocean with mild, humid winters (mean air temperature is 11 °C in January; average annual precipitation is 505.6 mm) and warm, dry summers (mean air temperature is 25 °C in August with almost no rainfall). The salt marshes in the study area are flooded twice a day by semi-diurnal mesotidal tides (tidal range [equinoctial mean] of 2.97 m; Figueroa et al., 2003). The bedrock in the Odiel and Tinto basins

primarily consists of Palaeozoic volcanic and sedimentary rocks rich in pyrite (FeS_2) and other sulphide minerals (Achterberg et al., 2003). Presently, the tidal marshes in the Odiel–Tinto Estuary are being polluted with metals coming from AMD (Beltrán et al., 2010; Santos Bermejo et al., 2003). These salt marshes also receive acid discharges and a significant radioactive impact from industrial point sources and their waste deposits (e.g. PG stacks; Guerrero et al., 2021), which also emit particles and gases with relatively high concentrations of radon and hydrogen fluoride—one of the most toxic gaseous compounds—to the atmosphere (López-Coto et al., 2014; Torres-Sánchez et al., 2019, 2020). Some of the salt marsh areas are affected by agrochemical runoff from surrounding agricultural lands (Barba-Brioso et al., 2010). The tidal regime plays a crucial role in the immobilisation and dispersion of pollutants (Hierro et al., 2014a), with bioavailable metals serving as an important source of sediment toxicity (Rosado et al., 2016; Sáenz et al., 2003).

Our first sampling area (A1) was located in the salt marshes on the right bank of the Tinto River at its tidal confluence, an area known locally as 'Estero del Rincon'. These marshes are located near the PG stacks and are predominately colonised by *Sarcocornia perennis* (Mill.) A. J. Scott, *Atriplex portulacoides* L., the exotic invasive cordgrass *Spartina densiflora* Brongn and isolated patches of native *Spartina maritima* (Curtis) Fernald (Fig. S1). The second salt marsh area (A2) was located on the left bank of the Tinto River, opposite A1, in an area that is mainly colonised by *S. perennis*, *A. portulacoides*, *S. maritima* and *S. densiflora* (Fig. S1). A3 was located to the south on the right bank of the 'Canal del Padre Santo', the main channel of the Odiel–Tinto Estuary. The area is colonised by *S. densiflora* and isolated patches of *S. maritima* (Fig. S1). Location A4 was located in the salt marshes near the Chemical Park of Huelva City. This area was ecologically restored in 1992 and is now primarily covered with continuous prairies of *S. maritima* (Fig. S1; Curado et al., 2014). The location for A5 was selected because it is an area highly polluted with metals coming from AMD. It is close to the mineral wastes of an abandoned foundry that extend over 12,600 m^2 and are exposed to rain and rising river levels during spring tides (Davila et al., 2019). The area is colonised by *A. portulacoides* and *S. densiflora*. A6 was located in salt marshes upstream of the Tinto River in an acidic area with high levels of metal pollution (Curado et al., 2010). This area is primarily colonised by *A. portulacoides*, *Phragmites australis* (Cav.) Trin. ex Steud. and *S. densiflora* (Fig. S1). Location A7 was in the estuary of the Piedras River. The sediments in the area are relatively unpolluted as there is a small catchment area relative to that of neighbouring, more polluted rivers and the area has not been affected by human activity such as mining (Lario et al., 2016). This area is colonised by different *Sarcocornia* taxa, *A. portulacoides* and sparse clumps of *S. maritima* and *S. densiflora* (Fig. S1). Geographical coordinates for each sampling point are supplied in the supplementary materials (Table S1).

2.2. Sediment sampling and characteristics

Representative samples of sediments (approx. 2.5×10^{-4} m^3) were collected directly from each salt marsh area (A1-A7) in March 2021, by taking 10 randomly selected samples 10 cm deep in each sample area, coinciding with the rooting zone of the halophytes present in the studied

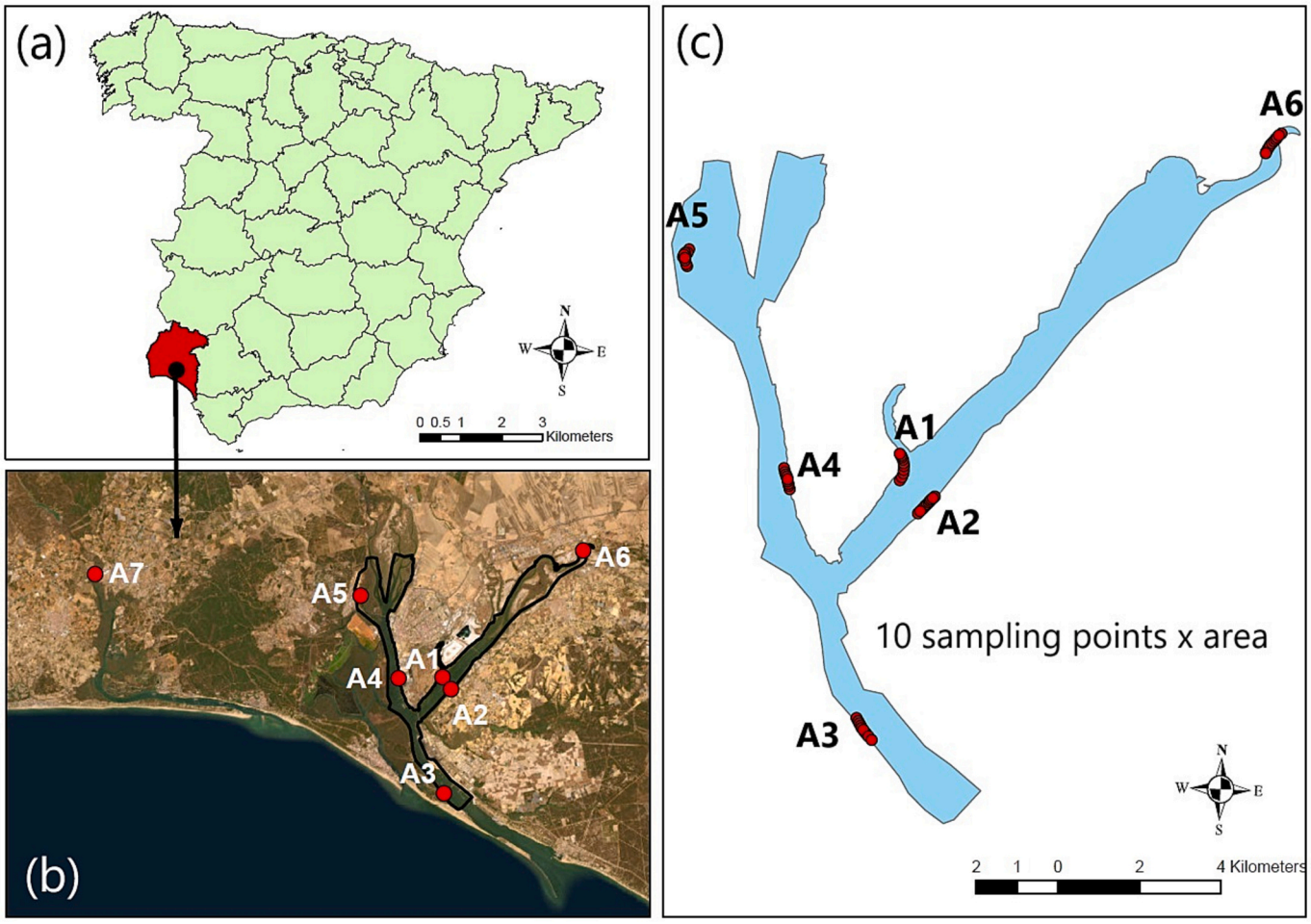

Fig. 1. (a) Location of study area in the Iberian Peninsula, (b) orthophotograph of the sampled salt marsh areas (red spots) in the Estuaries of Odiel-Tinto and Piedras Rivers, and (c) sampling locations of salt marsh sediments in the Odiel-Tinto Estuary(A1–6) and the Estuary of Piedras River (A7).

marshes. A total of 70 different sediment samples were collected. Samples were stored in a freezer at −20 °C until analysis. Within the study area, the main environmental driving factors for cation and anion mobility are pH under low salinity conditions and competitive desorption under high salinity conditions (Kerl et al., 2023). We recorded the pH, electrical conductivity (EC) as a measure of salinity, redox potential (Eh) and texture (i.e. percentages of sand, silt and clay) in the sediment samples. The pH, EC and redox potential of the sediment samples were measured in a 1:2 ratio of sediment to distilled water using a digital multimeter (LAQUA PC220. HORIBA Advanced Techno Co., Ltd.). The suspension was stirred at approximately 1200 rpm for 24 h before measuring the parameters of the supernatant solution. The corresponding value at 25 °C was obtained by temperature conversion of the results.

Sediment textures were analysed using the Bouyoucos hydrometer method (Bouyoucos, 1936). 50 g of dry soil and 100 mL of dispersant (5 % Calgon solution) were added to a flask and allowed to settle for a few minutes, before dispersing with a soil mixer running at approximately 500 rpm for 2 h. The soil suspension was then poured into a graduated cylinder, diluted to 1000 mL with distilled water and stirred with a stir bar. Hydrometer readings and temperature were recorded after 40 s and 2 h.

2.3. Chemical element concentrations in sediments

The sediment samples were analysed for the total concentrations (mg kg^{-1} dry weight) of 48 chemical elements (Table S1) at the University of Huelva. Soil samples were digested with HNO_3 at 220 °C in a microwave (UltraWAVE. Millestone Srl) and brought to 50 mL following digestion. Five replicates were conducted for each sample. Digestion blanks and a reference material were also included in duplicate. Major elements concentrations were determined by Inductively Coupled Plasma-Optical Emission Spectroscopy (ICP-OES; Agilent 5110), operating between 160 and 900 nm with external and periodic calibration ranged between 0.1 and 50 ppm, 0.1–100 ppm and 0.1–500 ppm. Detection and quantification limits were 0.1 ppm and 50 ppm, respectively. Trace elements concentrations were determined by Inductively Coupled Plasma-Mass Spectrometry (ICP-MS; Agilent 7700) with SPS4 autosampler and collision cell (He mode). Details on element concentration measurements and quality controls are supplied in the supplementary materials (Text S1).

2.4. Spatial distribution of chemical elements

The distribution of representative elements associated with the PG stacks, mineral wastes and AMD were spatially analysed. Maps of the spatial distribution of each of the chemical elements in the estuary were created using the inverse distance weighting (IDW) interpolation technique. This method gives greater weight to points close to the sampling location, assuming that the influence of the variable being represented decreases at greater distances from the sampling point (Lu and Wong, 2008). All spatial analyses were carried out with ArcGIS 10.5 software.

2.5. Data analyses

Statistical analyses were carried out using SPSS 15.0 (SPSS Inc., USA) and SigmaPlot 11.0 (Systat Software Inc., Germany). A significance level (α) of 0.05 was applied to all analyses and deviations were calculated as the standard error of the mean. Data were tested for homogeneity of variance and normality with Levene and Shapiro-Wilk tests, respectively. Sediment characteristics and chemical element concentrations were compared between salt marsh areas using parametric one-way ANOVAs (F-test) or non-parametric Kruskal–Wallis H-tests with a post-hoc Tukey test. The relationships between chemical element concentrations in the sediments of the seven sample salt marsh locations were analysed using a principal component analysis (PCA). The correlation matrix was analysed with 25 maximum iterations for convergence without rotation to extract independent PCA factors with eigenvalues >1. Regression factor scores from PCA for each sediment sample were compared between the seven salt marsh areas studied using Kruskal–Wallis H-tests with post-hoc Tukey tests.

3. Results

3.1. Sediment characteristics

Sediment characteristics differed significantly between the salt marsh areas (Table S2). Sediment pH was close to 7 for all salt marshes, with the exception of A6 (3.4 ± 0.1), located upstream of the Tinto River (Fig. 2a). Sediment EC was the highest in A1 near the PG stacks (33.8 ± 1.3 mS cm^{-1}) and the lowest in A6 (5.3 ± 0.3 mS cm^{-1}; Fig. 2b). Sediment Eh ranged from 245.6 ± 0.1 mV in A7 (Piedras River) to 352.5 ± 0.1 mV in A6 (Fig. 2c). Sediment texture was clayey in A1, A2, A5, A6 and A7, and mostly loamy and loamy-clay in A3 and A4 (Figs. 2d–f).

3.2. Sediment pollution signatures

Concentrations of the 48 chemical elements analysed differed significantly between the seven study salt marsh areas (Tables 1 and S3).

Eight factors, explaining 89.4 % of the variance, were obtained from the PCA for the concentration of chemical elements in the sediments. The first factor (PC1, explaining 33.9 % of total variance) was positively correlated with 20 chemical elements with factor loadings higher than +0.600, including Gd, U, Bi, Ba, Sr, Er, Ce, As, Mg, Zn, Cu and P (Table 2). The concentrations of these elements were highest in sediments from A1 and A2 (Fig. 3a and b). Regression factor scores for PC1 were significantly higher for A1 and A2 than for A4–7 (Fig. S2, Table S4). Using the IDW interpolation method, the spatial distribution of the concentration of elements such as P and U was clearly associated with the salt marsh sediments located at the edge of the PG stacks on the right bank of the main channel of the Tinto River (Fig. 4a and b). Concentrations of Gd and Ce were also the highest in the sediments located

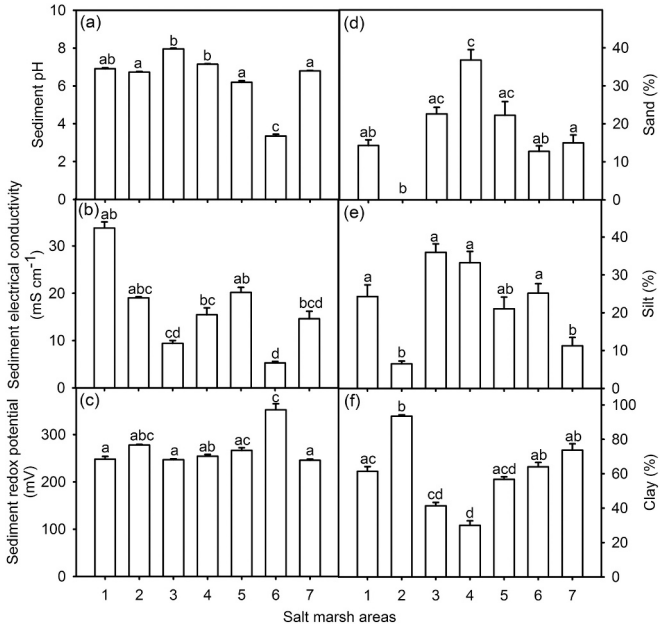

Fig. 2. Sediment (a) pH, (b) electrical conductivity, (c) redox potential and texture (% of (d) sand, (e) silt and (f) clay) in six salt marsh areas in the Odiel and Tinto Estuary (1–6) and one salt marsh in the Estuary of Piedras River (7) in Southwest Iberian Peninsula. Data are arithmetic means ± SEM (n = 10). Salt marsh areas are shown in Fig. 1. Different letters indicate significant differences between salt marsh areas (Tukey test, $p < 0.05$).

Table 1
Sediment concentrations (mg kg^{-1} DW) of forty-eight chemical elements in six salt marsh areas in the Odiel and Tinto Estuary (1–6) and one salt marsh in the Estuary of Piedras River (7) in Southwest Iberian Peninsula. Data are arithmetic means (up) ± SEM (down) ($n = 10$).

	As	Ba	Be	Bi	Ca	Cd	Ce	Co	Cr	Cs	Cu	Dy	Er	Eu	Fe	Ga	Gd	Ho	In	La	Li	Mg	Mn	Mo
Salt mash 1	866.5	430.8	0.9	17.9	7633.9	4.8	71.1	34.9	106.4	4.1	2944.9	7.7	4.2	1.9	107,338.6	17.2	10.6	1.3	2.5	38.4	106.3	10,488.2	369.6	9.0
	64.0	9.2	0.2	1.2	639.7	0.7	1.8	0.9	2.0	0.1	110.5	0.2	0.2	0.1	2523.4	0.3	0.3	0.1	0.1	1.6	1.1	179.0	28.5	0.4
Salt mash 2	632.2	407.6	2.7	17.2	4976.4	3.4	74.8	38.6	88.4	5.0	3067.7	7.0	3.8	2.1	91,131.0	18.4	10.3	1.4	2.1	35.8	129.8	10,333.6	358.8	8.5
	13.7	12.1	0.2	0.4	223.1	0.3	0.9	0.9	1.2	0.1	62.5	0.1	0.0	0.0	1513.2	0.2	0.1	0.0	0.0	0.6	2.9	128.9	36.1	0.7
Salt mash 3	421.2	202.8	0.6	6.8	15,655.3	1.0	49.4	31.6	46.6	1.5	1265.6	3.6	1.6	0.6	62,876.0	9.3	6.0	0.6	1.7	23.6	45.5	6749.5	444.5	7.2
	40.2	16.1	0.0	0.6	1826.5	0.2	2.2	1.8	2.8	0.2	85.1	0.3	0.2	0.0	4610.9	0.7	0.3	0.0	0.3	1.2	3.8	359.8	50.4	0.8
Salt mash 4	152.5	162.4	0.6	5.5	6195.2	0.6	33.4	20.3	48.8	1.0	1263.9	2.9	0.9	0.6	32,950.0	6.3	4.3	0.6	0.8	17.1	44.8	4819.0	307.7	6.6
	19.0	17.5	0.0	0.7	756.2	0.0	2.9	3.9	5.4	0.2	187.3	0.3	0.1	0.0	4286.0	0.8	0.4	0.0	0.2	1.5	4.8	577.2	66.9	2.1
Salt mash 5	16.7	25.2	0.9	4.6	4335.8	1.9	9.0	90.5	51.5	160.8	2333.0	1.2	0.6	11.2	173,693.2	10.8	1.3	3.8	2.6	68.8	60.4	7090.2	2140.6	0.6
	1.1	4.9	0.2	0.5	383.6	0.4	1.5	22.0	5.5	54.2	307.2	0.2	0.0	1.7	18,039.8	1.0	0.2	0.5	0.5	11.6	10.3	399.8	586.6	0.0
Salt mash 6	262.0	122.4	0.6	7.4	1112.0	0.6	13.6	6.9	57.0	199.3	536.9	1.0	0.6	1.6	158,327.3	11.4	1.5	0.7	2.3	17.9	25.5	4933.9	103.8	9.2
	87.6	41.5	0.0	1.0	63.6	0.0	3.7	0.4	0.9	18.2	79.7	0.2	0.0	0.4	4307.3	0.2	0.3	0.1	0.8	2.5	0.8	96.7	2.3	2.9
Salt mash 7	10.7	29.6	1.5	8.1	2274.1	0.6	7.2	16.1	75.2	178.2	46.2	0.6	0.6	6.2	42,557.4	18.9	0.6	1.5	0.8	70.8	45.8	7485.5	533.3	0.6
	4.0	1.2	0.3	0.4	149.7	0.0	0.3	2.0	2.0	5.0	3.9	0.0	0.0	0.3	1429.3	0.7	0.0	0.1	0.1	0.6	1.2	143.1	191.9	0.0
	Nb	Nd	Ni	P	Pb	Pr	Rb	S	Sc	Se	Sm	Sn	Sr	Tb	Th	Ti	Ti	Tl	Tm	U	V	Y	Yb	Zn
Salt mash 1	0.6	40.3	40.6	12,162.6	987.8	9.0	71.3	10,015.3	12.9	12.6	8.7	8.6	300.8	1.1	7.1	461.3	462.6	1.7	0.6	28.2	117.4	49.5	3.2	3471.5
	0.0	1.5	1.3	786.3	66.2	0.2	2.0	1590.2	0.3	0.7	0.3	0.4	23.2	0.1	0.1	14.1	14.6	0.2	0.0	1.1	1.1	2.5	0.1	109.3
Salt mash 2	0.6	40.2	46.5	7564.8	880.8	9.8	70.9	9998.8	13.2	11.7	9.0	9.6	226.0	1.4	7.7	475.7	474.0	1.8	0.6	12.6	109.6	39.5	3.0	3276.3
	0.0	0.5	0.4	233.1	21.5	0.1	1.3	1041.1	0.2	0.5	0.1	0.3	5.8	0.0	0.1	19.1	22.6	0.2	0.0	0.5	1.6	0.6	0.0	70.6
Salt mash 3	0.6	26.5	23.7	2495.3	386.7	5.4	39.2	3551.3	6.6	5.5	5.3	3.6	134.4	0.6	4.3	383.8	384.5	0.6	0.6	3.6	70.5	22.2	1.0	2303.2
	0.0	0.5	1.3	135.4	24.8	0.3	3.4	348.3	0.5	0.4	0.1	0.3	10.9	0.0	0.3	21.9	22.6	0.0	0.0	0.4	4.4	1.6	0.2	175.2
Salt mash 4	0.6	17.6	18.8	6319.6	245.8	3.8	27.0	2670.3	4.6	4.4	3.5	7.5	148.2	0.6	2.7	252.6	241.7	0.6	0.6	7.2	42.9	21.1	0.9	1149.8
	0.0	1.7	2.6	730.3	25.7	0.4	3.3	302.4	0.6	0.5	0.4	1.2	14.7	0.0	0.4	20.2	19.1	0.0	0.0	1.0	4.7	2.1	0.1	133.1
Salt mash 5	25.8	9.8	32.3	7857.7	945.6	41.6	163.3	10,713.6	8.4	28.1	2.0	4.2	35.9	6.0	29.7	231.8	212.2	993.2	3.0	0.0	88.7	8.3	0.6	2349.4
	7.4	1.4	4.6	1666.2	112.9	6.2	18.9	1705.7	0.9	3.1	0.3	0.3	5.6	0.5	3.6	21.9	21.0	114.1	0.4	0.0	7.5	0.7	0.0	285.2
Salt mash 6	8.5	7.0	19.6	3749.7	423.6	11.8	45.4	15,739.0	7.5	24.8	1.5	2.8	25.5	1.1	4.5	274.6	269.7	206.2	0.6	1.5	64.2	9.8	0.6	256.5
	2.7	1.6	0.8	184.2	58.6	0.7	3.3	654.9	0.2	6.5	0.3	0.7	7.0	0.2	0.6	15.4	15.2	75.3	0.0	0.6	2.3	1.2	0.0	37.3
Salt mash 7	1.5	5.7	36.6	1378.7	22.2	29.1	69.5	1357.3	11.1	73.6	1.1	0.6	16.0	3.8	2.1	265.4	293.0	24.5	1.0	0.0	97.3	20.1	0.6	103.5
	0.4	0.3	1.0	60.5	1.2	1.0	5.4	287.6	0.4	11.7	0.2	0.0	0.6	0.0	0.3	21.3	23.3	1.1	0.1	0.0	2.4	0.8	0.0	5.3

Table 2
Factor loadings of the individual variables obtained by a Principal Component Analysis (PCA) on chemical elements in sediments from the Joint Odiel and Tinto Estuary (Southwest Iberian Peninsula). Factor loadings > ± 0.600 are marked in bold. Kruskal-Wallis H-test for regression factor scores from PC for every sediment sample compared between locations (d. f. = 6).

Element	PC1	PC2	PC3	PC4	PC5	PC6	PC7	PC8
Gd	**0.958**	−0.161	−0.160	0.104	0.032	−0.061	−0.023	0.006
U	**0.886**	−0.224	−0.024	−0.127	−0.170	0.136	−0.130	0.141
Bi	**0.883**	−0.161	0.034	−0.312	0.017	−0.081	0.116	−0.103
Ba	**0.880**	−0.377	−0.113	−0.029	−0.047	−0.136	0.004	−0.075
Sr	**0.877**	−0.353	−0.105	0.094	0.036	0.031	−0.147	0.090
Er	**0.872**	0.412	−0.166	0.016	−0.069	−0.009	0.058	0.076
Ce	**0.869**	−0.407	−0.155	0.107	0.106	−0.100	−0.013	−0.031
As	**0.855**	−0.340	−0.099	−0.028	−0.163	0.084	0.125	−0.070
Y	**0.849**	−0.378	−0.067	−0.205	0.138	0.049	−0.032	0.126
Yb	**0.847**	0.458	−0.148	−0.016	−0.085	−0.070	0.018	0.061
Zr	**0.837**	0.242	−0.356	0.128	−0.197	−0.057	−0.037	−0.065
Ti	**0.834**	−0.137	−0.091	−0.013	0.192	−0.076	0.162	0.022
Mg	**0.829**	0.052	0.228	−0.175	0.281	−0.047	0.185	0.204
Zn	**0.755**	−0.270	0.332	0.325	0.178	−0.009	0.026	0.155
Cu	**0.734**	−0.219	0.505	0.243	0.161	−0.131	−0.120	−0.031
Sc	**0.701**	0.247	0.292	−0.434	0.263	−0.104	0.158	−0.074
V	**0.691**	0.233	0.400	−0.333	0.263	0.040	0.227	−0.017
Sn	**0.690**	−0.357	0.061	0.160	−0.087	−0.322	−0.225	0.064
Eu	**0.671**	−0.154	0.163	−0.222	−0.261	0.459	−0.051	0.217
P	**0.649**	−0.178	0.483	0.028	−0.085	0.108	−0.290	−0.105
Li	0.566	−0.229	−0.019	−0.092	−0.234	0.467	−0.265	0.160
Tm	0.090	**0.960**	−0.115	0.172	−0.096	0.051	−0.030	−0.030
Ho	0.132	**0.952**	−0.175	0.144	−0.107	0.043	−0.017	−0.013
In	0.197	**0.882**	−0.125	0.150	−0.196	0.011	0.098	0.129
Cr	0.464	**0.851**	−0.171	−0.078	−0.070	0.028	0.010	−0.001
Mo	0.270	**0.818**	−0.343	0.161	−0.233	0.010	0.016	−0.090
Ga	0.123	**0.788**	−0.217	0.131	−0.115	0.040	−0.026	−0.017
Cd	0.566	**0.754**	−0.037	0.072	−0.122	0.065	0.023	0.019
Dy	0.598	**0.726**	−0.271	0.148	−0.096	0.005	−0.021	0.018
Ni	0.617	**0.627**	0.157	−0.133	0.336	−0.075	0.010	−0.014
Tb	−0.240	0.396	0.242	−0.242	0.323	0.214	−0.008	0.310
Th	−0.066	0.072	**0.870**	0.297	0.049	0.001	−0.061	−0.090
Tl	−0.329	0.165	**0.845**	0.213	0.003	0.038	0.002	−0.021
Rb	0.053	0.419	**0.811**	0.127	0.152	0.022	0.006	0.037
Fe	−0.065	−0.032	**0.687**	0.097	−0.500	−0.143	0.379	0.082
Pb	0.598	−0.184	**0.682**	0.141	−0.097	−0.018	0.067	−0.096
Mn	−0.063	0.327	**0.661**	0.339	0.272	0.213	−0.239	−0.126
Co	0.170	0.487	0.579	0.387	0.268	0.147	−0.210	−0.111
Se	−0.359	0.469	0.082	**−0.629**	0.358	0.117	0.133	0.079
La	−0.273	0.098	0.043	**−0.608**	0.492	0.221	0.037	0.207
Ca	0.255	−0.299	−0.261	0.574	0.292	0.373	0.072	0.159
Nd	0.172	−0.261	−0.299	0.532	0.335	0.307	0.522	−0.093
S	0.079	−0.122	0.390	−0.104	**−0.602**	−0.294	0.450	0.095
Pr	0.345	−0.125	0.143	−0.276	−0.463	0.519	0.086	−0.234
Be	0.410	0.211	0.079	−0.247	0.359	−0.501	0.144	−0.326
Cs	−0.017	−0.008	0.429	−0.447	−0.363	0.490	0.173	−0.343
Sm	−0.036	−0.179	−0.304	0.534	0.322	0.335	0.557	−0.091
Nb	−0.365	0.115	0.478	0.214	−0.304	−0.194	0.224	0.499
Eigenvalues	16.256	9.086	6.299	3.509	2.997	2.101	1.617	1.047
Explained variance (%)	33.9	18.9	13.1	7.3	6.2	4.4	3.4	2.2
Kruskal-Wallis H-test	50.479	59.530	61.160	50.541	41.137	44.794	37.134	12.807
P	0.000	0.000	0.000	0.000	0.000	0.000	0.000	0.046

on the right and left banks of the Tinto River close to the PG stacks, however, relatively high concentrations of these two elements extended across a wide area along the main channel of the estuary (Fig. 4c).

The second principal component (PC2, explaining 18.9 % of variance) was positively correlated with 9 elements with factor loadings higher than +0.600, including Tm, Ho, Cr, Mo, Ga, Cd and Ni (Table 2). The concentrations of these elements were the highest in the sediments from A1 and A2 (Table 1, Fig. 3c). Regression factor scores for PC2 were the lowest for A1, A3 and A4 (Fig. S2).

PC3 explained 13.1 % of the variance and was positively correlated with 6 elements with factor loadings higher than +0.600 (Th, Tl, Rb, Fe, Pb and Mn; Table 2). Regression factor scores for PC3 were the highest for A5, which was close to an abandoned foundry (Fig. S2). High concentrations of Th were mostly associated with sediments close to the abandoned foundry (Fig. 4f); concentrations of Fe were also associated with the abandoned foundry but increased moving upstream along both the Odiel and Tinto Rivers (Fig. 3e and Fig. 4g). Concentrations of Pb were higher upstream in the Tinto River and downstream along the main channel of the estuary than in sediments located at intermediate locations in the Odiel and Tinto Rivers (Figs. 3f and 4h).

PC4 (explaining 7.3 % of variance) was negatively correlated with Se and La (Table 2). Its regression factor scores were the highest for A3 and A5 and the lowest for A7 (Fig. S2), where La and Se showed their maximum concentrations (Fig. 3g, Table 1). PC5 (explaining 6.2 % of variance) was negatively correlated with S concentrations (Table 2), and its regression factor scores were the lowest upstream in the Tinto River (A6; Fig. S2). Sulphur concentrations were highest in sediments located upstream in the Tinto River, and reduced gradually moving downstream towards the ocean (Figs. 3d and 4e). PC6 explained 4.4 % of the variance and was positively correlated with Pr and Cs and negatively with Be (Fig. 4d, Table 2). These two elements, Pr and Cs, had maximum concentrations in A5 and A6 (Fig. 3h). The regression factor scores for PC6

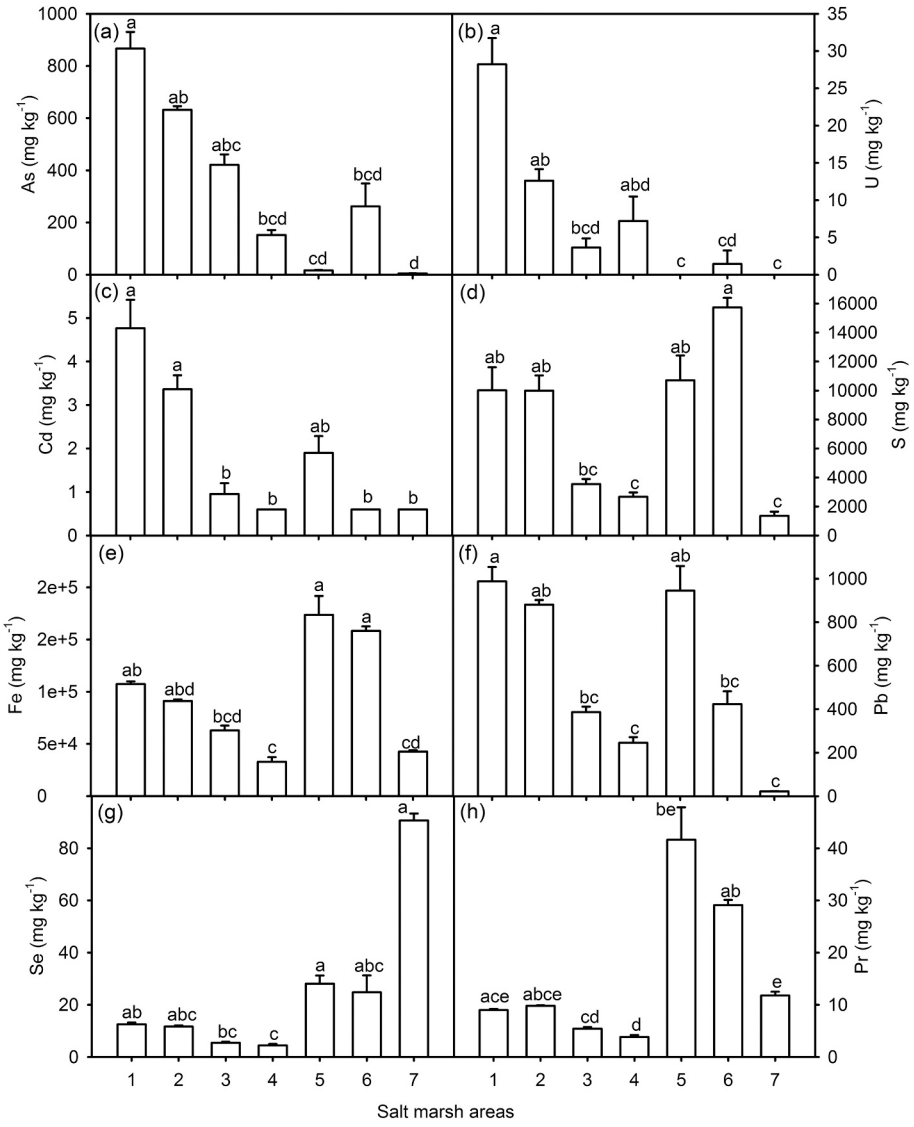

Fig. 3. Total concentrations (mg kg-1 DW) of (a) As, (b) U, (c) Cd, (d) S, € Fe, (f) Pb, (g) Se and (h) Pr in sediments from the Odiel-Tinto Estuary (1–6) and the Estuary of Piedras River (7) in Southwest Iberian Peninsula. Data are arithmetic means ± SEM (n = 10). Salt marsh areas are shown in Fig. 1. Different letters indicate significant differences between salt marsh areas (Tukey test, $p < 0.05$).

were the highest for A1 and A3 and the lowest for A2 (Fig. S2).

4. Discussion

By modelling the spatial distribution of 48 chemical elements in sediments from seven salt marsh areas across the Odiel–Tinto Estuary, we successfully identified three unique chemical signatures linked to specific pollution sources: in salt marsh sediments from AMD upstream of the Tinto River, in sediments located near PG waste piles and in sediments near an abandoned foundry.

Peak concentrations of 20 elements were found in sediments near the PG stacks (site A1). These elements were associated with PC1, which explained the greatest proportion of the data variance (34 %). Notably, most of these 20 elements have been previously documented in edge outflows and nanoparticles originating from PG stacks within the study area (Millán-Becerro et al., 2023; Pérez-López et al., 2016; Ruiz Cánovas et al., 2018; Silva et al., 2022). Among radionuclides, U-series isotopes possess the highest mobility within PG stacks (Pérez-Moreno et al., 2018). The majority of these 20 elements associated with sediments near the PG stacks, including Al, Cr, Fe, Pb and U, tend to precipitate under neutral seawater conditions (pH 6.9 ± 0.1) through co-precipitation and/or adsorption onto phosphate phases. Fluoride precipitation also contributes to their removal (Guerrero et al., 2020; Papaslioti et al., 2018). Additionally, elements like As, Cd, Co, Cr, Cu, Ni, Pb, U and Zn precipitate when the sediment pH exceeds 4 and Eh falls below +340 mV. This is facilitated by Fe-limited sulphide precipitation, particularly in organic-rich sediments with low Eh(DeLaune and Reddy, 2005; Guerrero et al., 2019; Hierro et al., 2014a; Pérez-López et al., 2011, 2018; Santos Bermejo et al., 2003). Consequently, a significant portion of the chemical elements present in acidic leachates from the PG stacks have the potential to precipitate and become immobilised within the surrounding fine-textured, near-neutral, oxidised (Eh 248 ± 6 mV) sediments.

The PG stacks are located in the estuarine zone where seawater meets the Tinto River. This zone is characterised by a sharp shift in water properties, with salty and neutral–basic ocean waters encountering acidic, brackish river water (Chica-Olmo et al., 2004). This meeting point leads to the neutralisation of acidic waters, causing the precipitation of chemical elements from both the PG stacks and those transported down the Tinto River. This phenomenon is reflected in a significant decrease in Cu concentrations in the water just downstream of the PG stacks (Chica-Olmo et al., 2004). Interestingly, arsenic

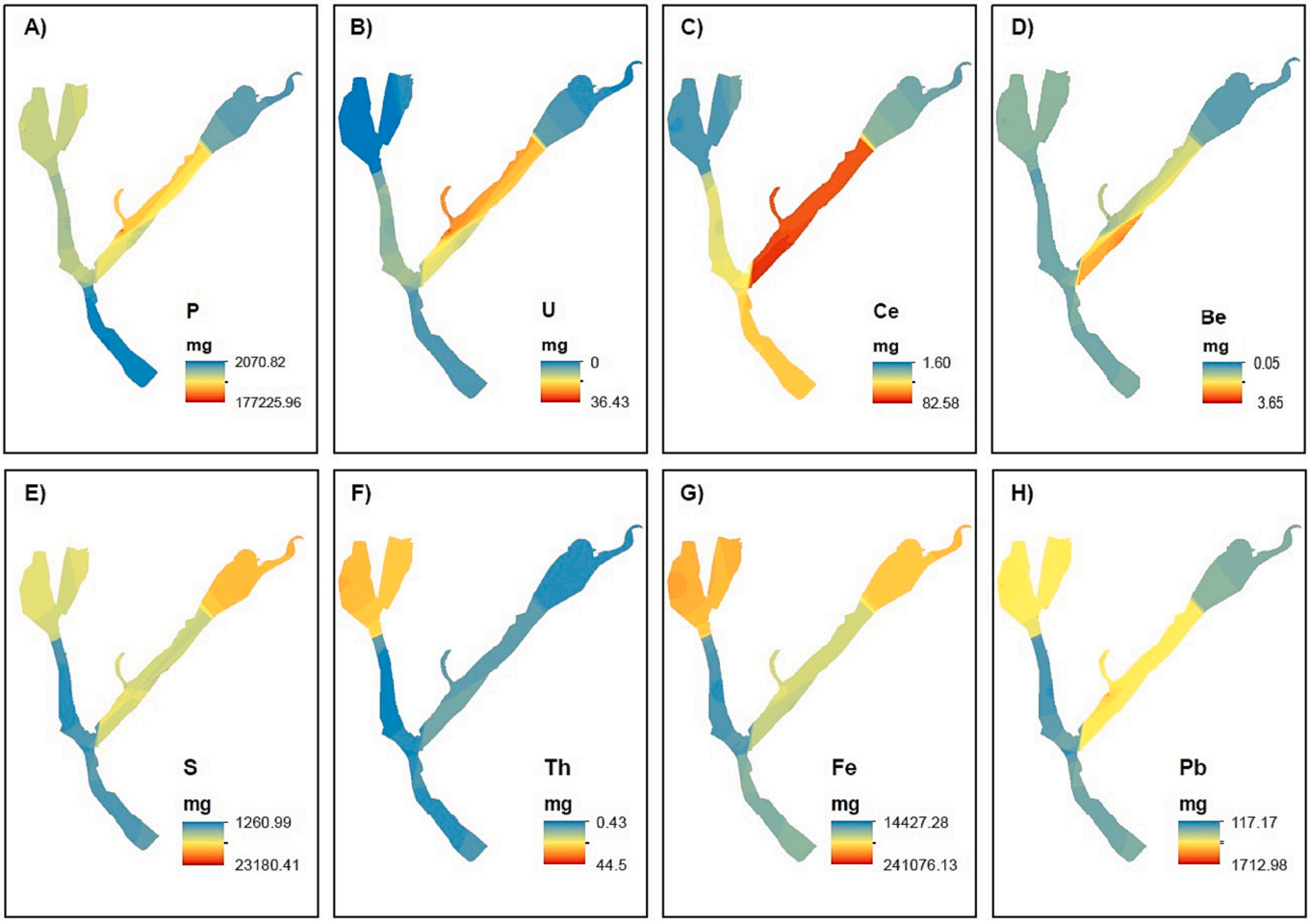

Fig. 4. Spatial distribution of representative chemical elements ((a) P, (b) U, (c) Gd, (d) Ce, (e) S, (f) Th, (g) Fe, and (h) Pb) in the Odiel-Tinto Estuary.

concentrations at the levels recorded in our study (866.5 ± 64.0 mg kg^{-1}) may show high ecotoxicity levels when accumulated in marsh sediments (Hwang et al., 2008).

Guerrero et al. (2019) suggested phosphorus as a suitable tracer to determine the impact of PG stacks on sediments. Phosphorus dissolves in the PG pore water as phosphoric acid, which is the main source of phosphoric acid for marshes, i.e. it is not associated with AMD or other sources of pollution. In addition to P, our study identified trace elements such as Gd, Bi, Ce and Zr as potential geochemical tracers. These elements exhibited relatively high concentrations, characteristic of the pollution signature of the PG stacks in the salt marsh sediments. Elements with the highest loadings in PC2 (Cd, Cr, Dy, Ga, Ho, Ni and Tm) showed the greatest sediment concentrations in salt marshes near the PG stacks on both banks of the Tinto River (A1 and A2). Some of these elements, particularly Cd and Ni, have a higher tendency to remain in solution when pH increases, compared to elements associated with PC1, with an average removal of around 60 % (Beltrán et al., 2010; Hierro et al., 2014a; Morillo et al., 2008; Sáenz et al., 2003).

Several chemical elements previously identified in PG stack outflows by Pérez-López et al. (2016), including major elements (Fe and S) and trace elements (Cd, Co, Pb and Ni), were not among those with the highest loadings in PC1, the principal component characterising the sediments near the PG stacks. However, Co, Fe and Pb exhibited the highest sediment concentrations—alongside Mn, Th, Tl and Rb—within the salt marshes closest to the abandoned foundry's mineral waste (site A5; Curado et al., 2014). Studies by Morillo et al. (2008), Beltrán et al. (2010), and Hierro et al. (2014b) have suggested that element precipitation, particularly that of Fe, is significant during rising tides in this area. Notably, elements typically associated with AMD, such as Co, Fe, Pb, Mn, Tl and Rb (da Silva et al., 2005; Fernández-Landero et al., 2023; Millan-Becerro et al., 2024) exhibited the highest loadings on PC3, a component explaining 13 % of the data variance across the estuary. This association suggests their utility as geochemical tracers for AMD pollution.

Our analysis revealed the highest total sulphur concentrations in upstream sediments in the Tinto River (site A6). These concentrations (15,739 ± 655 mg kg^{-1}) were 32 % higher than the second-highest value (site A5). Notably, sulphur was the only chemical element with a factor loading exceeding 0.600 in PC5, which explained 6 % of the data variance. This suggests that relatively high sulphur concentrations serve as a unique geochemical marker upstream in the highly polluted Tinto River Estuary. The low pH and high Eh in this environment, driven by extensive pyrite oxidation, promote the dissolution of large quantities of toxic elements and radionuclides (Mehdi et al., 2013).

Estuarine sediments in the Piedras River displayed relatively high concentrations of Se and La. These elements were strongly associated with PC4, explaining 7.3 % of the data variance. Alkaline soils are known to release more Se than acidic ones (Santos Bermejo et al., 2003). This aligns with the higher Se concentrations observed in the Piedras River salt marshes (site A7), as its hydrological basin is not impacted by AMD, unlike those of the Odiel and Tinto Rivers.

Two sampling sites (A2 and A7), situated near intensive strawberry cultivation in greenhouses exhibited the highest average beryllium concentrations (1.5–2.7 mg kg^{-1}). These values were over 40 % higher than those measured near the PG stacks (site A1), despite beryllium being identified as a trace element in these waste deposits (Silva et al.,

2022). Beryllium was associated with PC6, which explained 4 % of the data variance. Interestingly, PC6 clearly distinguished sediments near the PG stacks (site A1) from those across the Tinto River (site A2) with elevated beryllium. This suggests that beryllium may be a suitable geochemical marker for tracing the influence of intensive agriculture on the area's pollution profile. Given its widespread use in metal alloys, beryllium could potentially originate from the greenhouses' metal structures and become readily trapped in sediment (ATSDR, 2022).

Many studies have been conducted on the spatial distribution of heavy metals in other highly polluted locations providing important data for pollution management and future remediation (Dong et al., 2024; Liu et al., 2024; Sun et al., 2025). Our study characterises the sediment pollution signatures in a highly polluted Spanish estuary that has not yet been well researched. This characterisation allows us to differentiate between pollution sources including PG stacks, AMD in waste deposits and agricultural activities. This knowledge is valuable for developing integrated monitoring and pollution management plans, which can quantify and ultimately reduce the impacts of pollution from each source. The specific sediment pollution signatures identified in this study may be used as a reference to determine the impact of future interventions on existing pollution sources in the Odiel–Tinto Estuary. This study is critical for assessing the impact of the RESTORE 2030 plan, which is currently undergoing judicial review and being re-evaluated. Additionally, this study identified the sediment pollution signature of an abandoned foundry, which is located next to a residential area. The findings may also be used to evaluate future restoration plans for this area, which was declared contaminated by the Andalusian Government in 2007 (BOJA No. 168, 2007).

As the specific causes of the excess mortality rates in the Huelva area (Alguacil et al., 2014; Benach et al., 2003; Lopez-Abente et al., 2001) are known to be related to industrial and mining metal environmental pollution (Briffa et al., 2020), we believe that studying correlations between the original sources responsible for the pollutants accumulated in the sediments of the Huelva Estuary and mortality in Huelva is warranted from a public health perspective. Biomonitoring of the population and ecosystem's exposure to metals is also justified, as recommended by at least two different independent panels of scientific experts (Alguacil et al., 2014; Scientific committee, 2022).

5. Conclusions

We identified a specific pollution signature for PG stacks that distinguishes metal exposure from the other pollution sources in the Odiel–Tinto Estuary—AMD near mining waste deposits, pollution along the Tinto River and areas under intensive agricultural cultivation. The sediment pollution signature near the PG stacks was characterised by 20 elements such as Gd, U, As, Mg, Zn, Cy and P. Sediments near mining waste deposits specifically accumulated six elements, including Fe, Pb and Mn. The pollution signature in the sediment of the Tinto River was marked by high sulphur accumulation. Beryllium is a suitable marker for tracing the influence of intensive agriculture. These results provide a valuable tool for discriminating between different pollution sources, quantifying the most impacted areas of the salt marsh, assigning responsibility to the various polluting entities within the estuary, and setting a starting point to evaluate the impact of the RESTORE 2030 restoration plan for the Huelva estuary. These specific sediment pollution signatures may also be used as a reference to determine the impact of future interventions on existing pollution sources in other estuaries and marshes polluted with PG.

CRediT authorship contribution statement

Manuel Contreras-Llanes: Writing – review & editing, Writing – original draft, Visualization, Validation, Supervision, Resources, Methodology, Investigation, Conceptualization. **Vanessa Santos-Sánchez:** Writing – review & editing, Validation, Software, Formal analysis, Data curation. **Juan Alguacil:** Writing – review & editing, Visualization, Validation, Resources, Project administration, Methodology, Funding acquisition, Conceptualization. **Jesús M. Castillo:** Writing – review & editing, Writing – original draft, Visualization, Validation, Supervision, Software, Methodology, Investigation, Formal analysis, Data curation, Conceptualization.

Funding

This research was funded by the Andalusian Government, '2018 Special Action of the Andalusian Government: Support to the Huelva Phosphogypsum Experts Committee'; and by Huelva University local funds to support research groups during 2018 to 2023.

Declaration of competing interest

The authors declare the following financial interests/personal relationships which may be considered as potential competing interests: Juan Alguacil reports financial support was provided by Andalusian Government. If there are other authors, they declare that they have no known competing financial interests or personal relationships that could have appeared to influence the work reported in this paper.

Acknowledgments

We want to thank the technical advice and support from M.A. Garcia-Sevillano and J.L. Gomez-Ariza on how to proceed with the sample processing, and to Adrian Polonio for sample collection support. We thank the management of the Odiel Marshes Natural Park for its collaboration.

Appendix A. Supplementary data

Supplementary data to this article can be found online at https://doi.org/10.1016/j.scitotenv.2024.177715.

Data availability

Data will be made available on request.

References

Achterberg, E.P., Herzl, V.M.C., Braungardt, C.B., Millward, G.E., 2003. Metal behaviour in an estuary polluted by acid mine drainage: the role of particulate matter. Environ. Pollut. 121, 283–292. https://doi.org/10.1016/S0269-7491(02)00216-6.

Agency for Toxic. Substances and Disease Registry (ATSDR) and the Environmental Protection Agency (EPA), 2022. Toxicological Profile for Beryllium. U.S. Department of Health and Human Services. https://www.atsdr.cdc.gov/toxprofiles/tp4.pdf.

Alguacil, J., Ballester, F., Donado-Campos, J., Pollán, M., Rodríguez-Artalejo, F., 2014. Dictamen realizado por encargo del Defensor del Pueblo Andaluz sobre El exceso de mortalidad y morbilidad detectado en varias investigaciones en La Ría de Huelva. Grupo de Trabajo de la Sociedad Española de Epidemiología. Huelva. https://www.defensordelpuebloandaluz.es/sites/default/files/Huelva.pdf.

Barba-Brioso, C., Fernández-Caliani, J.C., Miras, A., Cornejo, J., Galán, E., 2010. Multi-source water pollution in a highly anthropized wetland system associated with the estuary of Huelva (SW Spain). Mar. Pollut. Bull. 60, 1259–1269. https://doi.org/10.1016/j.marpolbul.2010.03.018.

Beltrán, R., de la Rosa, J.D., Santos, J.C., Beltrán, M., Gómez-Ariza, J.L., 2010. Heavy metal mobility assessment in sediments from the Odiel River (Iberian Pyritic Belt) using sequential extraction. Environ. Earth Sci. 61, 1493–1503. https://doi.org/10.1007/s12665-010-0465-y.

Benach, J., Yasui, Y., Borrell, C., Rosa, E., Pasarín, M.I., Benach, N., Español, E., Martínez, J.M., Daponte, A., 2003. Examining geographic patterns of mortality: the atlas of mortality in small areas in Spain (1987-1995). Eur. J. Public Health 13 (2), 115–123. https://doi.org/10.1093/eurpub/13. 2.115.

Blasco, J., Sáenz, V., Gómez-Parra, A., 2000. Heavy metal fluxes at the sediment–water interface of three coastal ecosystems from south-west of the Iberian Peninsula. Sci. Total Environ. 247, 189–199. https://doi.org/10.1016/S0048-9697(99)00490-8.

BOJA No. 168, 2007. Resolution of August 7, 2007, of the General Directorate of Prevention and Environmental Quality, declaring two plots of the Partial Residential Plan No. 9 of Aljaraque (Huelva) as contaminated soil. Bulletin number 168, 80-82. Official Gazette of the Government of Andalusia - BOJA. https://www.juntadeandalucia.es/boja/2007/168/9.

Borrego, J., Morales, J., de la Torre, M., Grande, J., 2022. Geochemical characteristics of heavy metal pollution in surface sediments of the Tinto and Odiel river estuary (southwestern Spain). Environ. Geol. 41, 785–796. https://doi.org/10.1007/s00254-001-0445-3.

Bouyoucos, G.J., 1936. Directions for making mechanical analysis of soils by the hydrometer method. Soil Sci. 4, 225–228. https://doi.org/10.1097/00010694-193609000-00007.

Briffa, J., Sinagra, E., Blundell, R., 2020. Heavy metal pollution in the environment and their toxicological effects on humans. Heliyon 6 (9), e04691. https://doi.org/10.1016/j.heliyon.2020.e04691.

Carro, B.M., Reyes, A., Morales, J.A., Borrego, J., 2021. Application of the comparison of multibeam echo-sound records to the study of stability of a toxic waste stockpile located on the margin of a tidal system: Tinto estuary, Huelva, SW Spain. Remote Sens. 13, 4364. https://doi.org/10.3390/rs13214364.

Chica-Olmo, M., Rodriguez, F., Abarca, F., Rigol-Sanchez, J.P., deMiguel, E., Gomez, J. A., Fernandez-Palacios, A., 2004. Integrated remote sensing and GIS techniques for biogeo- chemical characterization of the Tinto-Odiel estuary system, SW Spain. Environ. Geo. 45, 834–842. https://doi.org/10.1007/s00254-003-0943-6.

Curado, G., Rubio-Casal, A.E., Figueroa, E., Castillo, J.M., 2010. Germination and establishment of the invasive cordgrass Spartina densiflora in acidic and metal polluted sediments of the Tinto River. Mar. Pollut. Bull. 60, 1842–1848. https://doi.org/10.1016/j.marpolbul.2010.05.022.

Curado, G., Rubio-Casal, A.E., Figueroa, E., Castillo, J.M., 2014. Plant zonation in restored, nonrestored, and preserved Spartina maritima salt marshes. J. Coast. Res. 30, 629–634. https://doi.org/10.2112/JCOASTRES-D-12-00089.1.

Davila, J.M., Sarmiento, A.M., Santisteban, M., Luís, A.T., Fortes, J.C., Diaz-Curiel, J., Valbuena, C., Grande, J.A., 2019. The UNESCO national biosphere reserve (Marismas del Odiel, SW Spain): an area of 18,875 ha affected by mining waste. Environ. Sci. Pollut. Res. 26, 33594–33606. https://doi.org/10.1007/s11356-019-06438-7.

DeLaune, R.D., Reddy, K.R., 2005. Redox Potential. In: Hillel, Daniel (Ed.), Encyclopedia of Soils in the Environment. Elsevier, pp. 366–371. ISBN 9780123485304. https://doi.org/10.1016/B0-12-348530-4/00212-5.

Dong, Y., Lu, H., Lin, H., 2024. Comprehensive study on the spatial distribution of heavy metals and their environmental risks in high-sulfur coal gangue dumps in China. Journal of Environ- mental Sciences 136, 486–497. https://doi.org/10.1016/j.jes.2022.12.023.

Elbaz-Poulichet, F., Morley, N., Cruzado, A., Velásquez, Z., Achterberg, E., Braungardt, C., 1999. Trace metal and nutrient distribution in an extremely low pH (2.5) river–estuarine system, the ria of Huelva (south–West Spain). Sci. Total Environ. 227, 73–83. https://doi.org/10.1016/S0048-9697(99) 00006-6.

Fernández-Landero, S., Fernández-Caliani, J.C., Giráldez, M.I., Morales, E., Barba-Brioso, C., González, I., 2023. Soil contaminated with hazardous waste materials at Rio Tinto mine (Spain) is a persistent secondary source of acid and heavy metals to the environment. Minerals 13, 456. https://doi.org/10.3390/min13040456.

Figueroa, M.E., Castillo, J.M., Redondo-Gómez, S., Luque, T., Castellanos, E.M., Nieva, F. J., Luque, C., Rubio-Casal, A.E., Davy, A.J., 2003. Facilitated invasion by hybridization of Sarcocornia species in a salt-marsh succession. J. Ecol. 91, 616–626. https://doi.org/10.1046/j.1365-2745.2003.00794.x.

González, F., 2022. InSAR-based mapping of ground deformation caused by industrial waste disposals: the case study of the Huelva phosphogypsum stack, SW Spain. Bull. Eng. Geol. Environ. 81, 304. https://doi.org/10.1007/s10064-022-02809-6.

Guerrero, J.L., Gutiérrez-Álvarez, I., Mosqueda, F., Olías, M., García-Tenorio, R., Bolívar, J.P., 2019. Pollution evaluation on the salt-marshes under the phosphogypsum stacks of Huelva due to deep leachates. Chemosphere 230, 219–229. https://doi.org/10.1016/j.chemosphere.2019.04.212.

Guerrero, J.L., Pérez-Moreno, S.M., Gutiérrez-Álvarez, I., Gázquez, M.J., Bolívar, J.P., 2020. Behaviour of heavy metals and natural radionuclides in the mixing of phosphogypsum leachates with seawater. Environ. Pollut. 268, 115843. https://doi.org/10.1016/j.envpol.2020.115843.

Guerrero, J.L., Gutiérrez-Álvarez, I., Hierro, A., Pérez-Moreno, S.M., Olías, M., Bolívar, J. P., 2021. Seasonal evolution of natural radionuclides in two rivers affected by acid mine drainage and phosphogypsum pollution. CATENA 197, 104978. https://doi.org/10.1016/j.catena.2020.104978.

Hierro, A., Olías, M., Ketterer, M.E., Vaca, F., Borrego, J., Cánovas, C.R., Bolívar, J.P., 2014a. Geochemical behavior of metals and metalloids in an estuary affected by acid mine drainage (AMD). Environ. Sci. Pollut. Res. Int. 21, 2611–2627. https://doi.org/10.1007/s11356-013-2189-5.

Hierro, A., Olías, M., Cánovas, C.R., Martín, J.E., Bolívar, J.P., 2014b. Trace metal partitioning over a tidal cycle in an estuary affected by acid mine drainage (Tinto estuary, SW Spain). Sci. Total Environ. 497–498, 18–28. https://doi.org/10.1016/j.scitotenv.2014.07.070.

Hwang, H.M., Green, P.G., Young, T.M., 2008. Tidal salt marsh sediment in California, USA: part 3. Current and historic toxicity potential of contaminants and their bioaccumulation. Chemosphere 71, 2139–2149. https://doi.org/10.1016/j.chemosphere.2008.01.005.

Kerl, C.F., Basallote, M.D., Käberich, M., Oldani, E., Cerón Espejo, N.P., Colina Blanco, A. E., Ruiz Cánovas, C., Nieto, J.M., Planer-Friedrich, B., 2023. Consequences of sea level rise for high metal(loid) loads in the Ría of Huelva estuary sediments. Sci. Total Environ. 873, 162354. https://doi.org/10.1016/j.scitotenv.2023.162354.

Lario, J., Alonso-Azcárate, J., Spencer, C., Zazo, C., Goy, J.L., Cabero, A., Dabrio, C.J., Borja, F., Borja, C., Civis, J., García-Ródriguez, M., 2016. Evolution of the pollution in the Piedras River Natural Site (Gulf of Cadiz, southern Spain) during the Holocene. Environ. Earth Sci. 75, 481. https://doi.org/10.1007/s12665-016-5344-8.

Leistel, J.M., Marcoux, E., Thieblemont, D., Quesada, C., Sanchez, A., Almodovar, G.R., Pascual, E., Saez, R., 1998. The volcanic-hosted massive sulphide deposits of the Iberian Pyrite Belt. Miner. Deposita 33, 2–30. https://doi.org/10.1007/s001260050130.

Li, C., Wang, H., Liao, X., Xiao, R., Liu, K., Bai, J., Li, B., He, Q., 2022. Heavy metal pollution in coastal wetlands: a systematic review of studies globally over the past three decades. J. Hazard. Mater. 424 Part A, 127312. https://doi.org/10.1016/j.jhazmat.2021.127312.

Lieberman, R.N., Izquierdo, M., Córdoba, P., Moreno Palmerola, N., Querol, X., Sánchez de la Campa, A.M., Font, O., Cohen, H., Knop, Y., Torres-Sánchez, R., Sánchez-Rodas, D., Muñoz-Quiros, C., de la Rosa, J.D., 2020. The geochemical evolution of brines from phosphogypsum deposits in Huelva (SW Spain) and its environmental implications. Sci. Total Environ. 700, 134444. https://doi.org/10.1016/j.scitotenv.2019.134444.

Liu, H., Zeng, W., He, M., 2024. Distribution, sources, contamination, and risks of toxic metals in Zijiang River, a typical tributary of the midstream of the Yangtze River in China. Journal of Environmental Sciences. https://doi.org/10.1016/j.jes.2023.12.030. In Press, Corrected Proof.

Lopez-Abente, G., Pollán, M., Escolar, A., Errezola, M., Abraira, V., 2001. Atlas of cancer morta-lity and other causes of death in Spain 1978-1992. In: Instituto de Salud Carlos III (ISCIII). Centro Nacional de Epidemiología (CNE), Madrid. http://hdl.handle.net/20.500.12105/4953.

López-Coto, I., Mas, J.L., Vargas, A., Bolívar, J.P., 2014. Studying radon exhalation rates variability from phosphogypsum piles in the SW of Spain. J. Hazard. Mater. 280, 464–471. https://doi.org/10.1016/j.jhazmat.2014.07.025.

Lu, G.Y., Wong, D.W., 2008. An adaptive inverse-distance weighting spatial interpolation technique. Comput. Geosci. 34, 1044–1055. https://doi.org/10.1016/j.cageo.2007.07.010.

Martínez-Beneito, M.A., Botella-Rocamora, P., Corpas-Burgos, F., Vergara-Hernández, C., Pérez-Panadés, J., Perpiñán-Fabuel, H., 2024. Atlas Nacional de Mortalidad en España (ANDEES). Fundación FISABIO y Dirección General de Salud Pública de la Generalitat Valenciana, Valencia. http://andees.fisabio.san.gva.es/.

Mehdi, Y., Hornick, J.L., Istasse, L., Dufrasne, I., 2013. Selenium in the environment, metabolism and involvement in body functions. Molecules 18, 3292–3311. https://doi.org/10.3390/molecules18033292.

Millán-Becerro, R., Pérez-López, R., Cánovas, C.R., Macías, F., León, R., 2023. Phosphogypsum weathering and implications for pollutant discharge into an estuary. J. Hydrol. 617, 128943. https://doi.org/10.1016/j.jhydrol.2022.128943.

Millan-Becerro, R., León, R., Romero-Matos, J., Moreno-González, R., Pérez-López, R., 2024. Towards circular and sustainable restoration of a deeply polluted river basin: the Odiel River catchment (SW Spain). Sci. Total Environ. 907, 168078. https://doi.org/10.1016/j.scitotenv.2023.168078.

Morillo, J., Usero, J., Rojas, R., 2008. Fractionation of metals and as in sediments from a biosphere reserve (Odiel salt marshes) affected by acidic mine drainage. Environ. Monit. Assess. 139, 329–337. https://doi.org/10.1007/s10661-007-9839-3.

Nie, J., Feng, H., Witherell, B.B., Alebus, M., Mahajan, M.D., Zhang, W., Yu, L., 2018. Assess- ment, and treatment of nutrient (N and P) pollution in Rivers, estuaries, and coastal waters. Curr. Pollut. Rep. 4, 154–161. https://doi.org/10.1007/s40726-018-0083-y.

Papaslioti, E.M., Pérez-López, R., Parviainen, A., Sarmiento, A.M., Nieto, J.M., Marchesi, C., Delgado-Huertas, A., Garrido, C.J., 2018. Effects of seawater mixing on the mobility of trace elements in acid phosphogypsum leachates. Mar. Pollut. Bull. 127, 695–703. https://doi.org/10.1016/j. marpolbul.2018.01.001.

Pérez-López, R., Nieto, J.M., López-Coto, I., Aguado, J.L., Bolívar, J.P., Santisteban, M., 2010. Dynamics of contaminants in phosphogypsum of the fertilizer industry of Huelva (SW Spain): from phosphate rock ore to the environment. Appl. Geochem. 25, 705–715. https://doi.org/10.1016/j.apgeochem.2010.02.003.

Pérez-López, R., Castillo, J., Sarmiento, A.M., Nieto, J.M., 2011. Assessment of phosphogypsum impact on the salt-marshes of the Tinto river (SW Spain): role of natural attenuation processes. Mar. Pollut. Bull. 62, 2787–2796. https://doi.org/10.1016/j.marpolbul.2011.09.008.

Pérez-López, R., Macías, F., Ruiz Cánovas, C., Sarmiento, A.M., Pérez-Moreno, S.M., 2016. Pollutant flows from a phosphogypsum disposal area to an estuarine environment: an insight from geochemical signatures. Sci. Total Environ. 553, 42–51. https://doi.org/10.1016/j.scitotenv.2016. 02.070.

Pérez-López, R., Carrero, S., Cruz-Hernández, P., Asta, M.P., Macías, F., Cánovas, C.R., Guglieri, C., Nieto, J.M., 2018. Sulfate reduction processes in salt marshes affected by phosphogypsum: geochemical influences on contaminant mobility. J. Hazard. Mater. 350, 154–161. https://doi.org/10.1016/j.jhazmat.2018.02.001.

Pérez-López, R., Millán-Becerro, R., Basallote, M.D., Carrero, S., Parviainen, A., Freydier, R., Macías, F., Cánovas, C.R., 2023. Effects of estuarine water mixing on the mobility of trace elements in acid mine drainage leachates. Mar. Pollut. Bull. 187, 114491. https://doi.org/10.1016/j.marpolbul.2022.114491.

Pérez-Moreno, S.M., Gázquez, M.J., Pérez-López, R., Vioque, I., Bolívar, J.P., 2018. Assessment of natural radionuclides mobility in a phosphogypsum disposal area. Chemosphere 211, 775–783. https://doi.org/10.1016/j.chemosphere.2018.07.193.

Rentería-Villalobos, M., Vioque, I., Mantero, J., Manjón, G., 2010. Radiological, chemical and morphological characterizations of phosphate rock and phosphogypsum from phosphoric acid factories in SW Spain. J. Hazard. Mater. 181, 193–203. https://doi.org/10.1016/j.jhazmat.2010.04.116.

RESTORE2030, 2020. Environmental restoration project of the Huelva phosphogypsum stacks (RESTORE2030) (accessed 23 June 2024). https://restore2030.com/.

Rosado, D., Usero, J., Morillo, J., 2016. Assessment of heavy metals bioavailability and toxicity toward Vibrio fischeri in sediment of the Huelva estuary. Chemosphere 153, 10–17. https://doi.org/10.1016/j.chemosphere.2016.03.040.

Ruiz Cánovas, C., Macías, F., Pérez López, R., Nieto, J.M., 2018. Mobility of rare earth elements, yttrium and scandium from a phosphogypsum stack: environmental and

economic implications. Sci. Total Environ. 618, 847–857. https://doi.org/10.1016/j.scitotenv.2017.08.220.

Sáenz, V., Blasco, J., Gómez-Parra, A., 2003. Speciation of heavy metals in recent sediments of three coastal ecosystems in the Gulf of Cadiz, Southwest Iberian Peninsula. Environ. Toxicol. Chem. 22, 2833–2839. https://doi.org/10.1897/02-448.

Santos Bermejo, J.C., Beltrán, R., Gómez Ariza, J.L., 2003. Spatial variations of heavy metals contamination in sediments from Odiel river (Southwest Spain). Environ. Int. 29, 69–77. https://doi.org/10.1016/S0160-4120(02)00147-2.

Scientific committee, 2022. Inform of the cientific committee of national experts coordinated from Huelva University about the RESTORE 2030 plan (accessed 20 June 2024). http://mesadelaria.es/documentos/Informe_280722_C_Expertos-Agosto2022.pdf.

da Silva, E.F.D., Fonseca, E., Matos, J., Patinha, C., Reis, P., Santos Oliveira, J.M., 2005. The effect of unconfined mine tailings on the geochemistry of soils, sediments and surface waters of the lousal area (Iberian Pyrite Belt, Southern Portugal). Land Degrad. Develop. 16, 213–228. https://doi.org/10.1002/ldr.659.

Silva, L.F.O., Oliveira, M.L.S., Crissien, T.J., Santosh, M., Bolivar, J.P., Shao, L., Dotto, G. L., Gasparotto, J., Schindler, M., 2022. A review on the environmental impact of phosphogypsum and potential health impacts through the release of nanoparticles. Chemosphere 286, 131513. https://doi.org/10.1016/j.chemosphere.2021.131513.

Sun, Y., Zhang, X., Peng, H., Zhou, W., Jiang, A., Zhou, F., Wang, H., Zhang, W., 2025. Develop- ment of a coupled model to simulate and assess arsenic contamination and impact factors in the Jinsha River Basin, China. Journal of Environmental Sciences 147, 50–61. https://doi.org/10.1016/j.jes. 2023.09.038.

Torres-Sánchez, R., Sánchez-Rodas, D., Sánchez de la Campa, A.M., Kandler, K., Schneiders, K., de la Rosa, J.D., 2019. Geochemistry and source contribution of fugitive phosphogypsum particles in Huelva, (SW Spain). Atmos. Res. 230, 104650. https://doi.org/10.1016/j.atmosres.2019.104650.

Torres-Sánchez, R., Sánchez-Rodas, D., Sánchez de la Campa, A.M., de la Rosa, J.D., 2020. Hydrogen fluoride concentrations in ambient air of an urban area based on the emissions of a major phosphogypsum deposit (SW, Europe). Sci. Total Environ. 714, 136891. https://doi.org/10.1016/j.scitotenv.2020.136891.